Rinta-Paavola, Aleksi; Hostikka, Simo

A Model for Pyrolysis and Oxidation of Two Common Structural Timbers

Published in:
Proceedings of the I Forum Wood Building Baltic, 2019

Published: 01/03/2019

Document Version
Publisher's PDF, also known as Version of record

Please cite the original version:
Rinta-Paavola, A., & Hostikka, S. (2019). A Model for Pyrolysis and Oxidation of Two Common Structural Timbers. In T. Kalamees, A. Just, M. Semjonov, A. Teder, & M. Deemant (Eds.), *Proceedings of the I Forum Wood Building Baltic, 2019* Tallinn University of Technology.
https://www.ttu.ee/public/k/Konverentsikeskus/A_Model_for_Pyrolysis_and_Oxidation_of_Two_Common_Structural_Timbers.pdf

A Model for Pyrolysis and Oxidation of Two Common Structural Timbers

Aleksi Rinta-Paavola
Aalto University
Espoo, Finland
e-mail: aleksi.rinta-paavola@aalto.fi

Simo Hostikka
Aalto University
Espoo, Finland
e-mail: simo.hostikka@aalto.fi

A Model for Pyrolysis and Oxidation of Two Common Structural Timbers

Abstract

The reduced cross section method for the calculation of timber structures' fire resistance is based on empirical and numerical assessment of charring propagation. The current work aims to construct a model for the pyrolysis and oxidation of spruce and pine woods to allow coupled simulations of cross section reduction and burning rate in fire models. A pyrolysis model for these woods is formulated based on thermogravimetric analysis (TGA), and supported by heat of pyrolysis and heat of combustion measurements by differential scanning calorimetry (DSC) and microscale combustion calorimetry (MCC), respectively. The results from small scale measurements (TGA, DSC and MCC) are consistent with each other. Therefore, heat of pyrolysis and heat of combustion was determined for the wood primary components by fitting a simulation into these experimental results. As a future work, cone calorimeter experiments are performed to optimize material properties and validate the model, and necessity of introducing an oxidation model is examined.

Key words: Charring; Pine wood; Pyrolysis modelling; Spruce wood

1. Introduction

Performance-based design of the timber structures' fire resistance is often based on the reduced cross section, and thus relying on empirical and numerical assessment of charring propagation. Coupling the charring propagation with fire conditions requires the use of numerical fire simulations, for which the heat release rate (HRR) is the most important boundary condition (Östman et al., 2017). This coupling means that the fire development is not prescribed but rather predicted using a pyrolysis model that simultaneously predicts charring and production of flammable gases (Matala et al., 2008). However, validated pyrolysis models for the wood species of Nordic structural timber are not readily available.

The current work aims to address this by providing a model for pyrolysis and oxidation of Norway spruce and Scots pine, the two most common structural timbers in Finland. The model provides a chemical kinetics -based estimate of pyrolysis and oxidation rates of the wood primary components and oxidation rate of the resultant char. With known heats of combustion of produced volatiles and heats of oxidation for virgin wood and char, HRR is calculated from the reaction rate. The model is intended as a solid phase HRR boundary condition in computational fluid dynamics –based fire simulators, such as Fire Dynamics Simulator (FDS). Model validation by cone calorimetry is planned as a future work.

2. Methods

2.1. Materials

The experiments were performed on samples of Norway spruce (Picea abies) and Scots pine (Pinus sylvestris) woods with measured average dry densities of 408 kg/m3 and 493 kg/m3, respectively. The chemical composition of spruce and pine woods are assumed as reported by Sjöström (1981), both consisting of roughly 28 % hemicellulose, 40 % cellulose and 27 % lignin by weight. Extractives account for <3.5 % while ash for <1 %.

2.2. Experimental

TA Instruments Q500 equipment was employed in thermogravimetric analyses (TGA) under an inert atmosphere (nitrogen) and in air. Four heating rates (2, 5, 10 and 20 K/min) were used and the runs were terminated at 600 °C (air) or at 800 °C (nitrogen).

Differential scanning calorimetry(DSC) is employed to measure the heat of pyrolysis and specific heat capacity of wood, using either Mettler Toledo DSC2 or DSC820 equipment,

respectively. All experiments are conducted under nitrogen. Heat of pyrolysis is measured from 25 to 500 °C with a heating rate of 20 K/min both with open and closed sample cups, with a small hole pierced to the lid. Secondary reactions lead to more exothermic heat of pyrolysis in the latter case (Rath et al., 2003). The specific heat was measured comparing to a sapphire standard at 10 K/min from 0 to 300 °C.

Heat release rate (HRR) of wood samples as a function of temperature was measured by pyrolysis combustion flow calorimetry (Lyon and Walters, 2004). Measurements were done with a microscale combustion calorimeter (MCC), using Govmark MCC-2 equipment. Experiments in both nitrogen and air were conducted (ASTM D7309, Method A or Method B, respectively) from 75 to 750 °C with heating rates of 20 and 60 K/min.

In TGA and MCC tests the samples were either small chips or sawdust whether the test is carried out in nitrogen or in air, respectively. All DSC samples were of sawdust. A milligram-order sample size is employed in these tests. TGAs for sawdust and solid chips in nitrogen were confirmed to be similar.

The cone calorimeter tests are conducted in a ventilation controlled cone calorimeter manufactured by Fire Testing Technology. The conical heater and load cell are inside a chamber with adjustable nitrogen and air inflows to control the atmosphere. The current experiments are conducted in pure nitrogen. 10 by 10 cm samples of pine and spruce with thicknesses of 1 and 2 cm were examined under heat flux levels of 35 and 50 kW/m^2. Since the current set-up allows only measurement of mass but not HRR, experiments in oxidative atmospheres are excluded for now.

Thermal conductivity of both woods in room temperature was measured with the transient plane source method (Log and Gustafsson, 1995), using HotDisk TPS2500 S equipment with 3.189 mm Kapton sensor. The sensor was placed between two 20 mm cubes cut from the same piece of wood. Sample conditioning was at 20 °C and 45 % relative humidity.

2.3. Reaction scheme

This work uses the scheme of parallel reactions where each wood component pyrolyzes independently, to allow for detailed analysis of decomposition throughout the entire temperature range. Many authors consider only reactions of three distinct primary components of hemicellulose, cellulose and lignin (e.g. Grønli, 1996; Hostikka and Matala, 2017). However, inclusion of extractives decomposition proved necessary to model mass loss onset correctly. Grønli et al. (2002) argue for its importance in softwoods, whereas for hardwoods the three components are often adequate. Therefore, this work employs the reaction scheme of Figure 1.

$$extractives \rightarrow char_e + volatiles$$

$$hemicellulose \rightarrow char_{hc} + volatiles$$

$$cellulose \rightarrow char_c + volatiles$$

$$lignin \rightarrow char_l + volatiles$$

Figure 1 The pyrolysis reaction scheme employed in this work.

2.4. Numerical

Numerical pyrolysis simulations were carried out using the pyrolysis solver of Fire Dynamics Simulator (FDS) version 6.5.2 (McGrattan et al., 2012). FDS is a Computational Fluid Dynamics model, which solves numerically Navier-Stokes equations for low Mach number, fire-driven flows, and models turbulence by Large Eddy Simulation. It also contains models for heat transfer and pyrolysis in solids. The mass concentration of component *a* changes according to the solid phase conservation equation.

$$\frac{\partial}{\partial t}\left(\frac{\rho_{s,\alpha}(x)}{\rho_s(0)}\right) = -\sum_{\beta=1}^{N_{r,\alpha}} r_{\alpha\beta}(x) + S_\alpha(x) \quad (1)$$

Where: $\rho_{s,a}$ mass concentration of component *a*
ρ_s density of the solid material mixture

x distance from the material surface
$N_{r,a}$ the number of reactions for component a
$r_{a\beta}(x)$ reaction rate of the β:th reaction of component a
S_a production rate of component a from other reactions

The mass concentration of component a with mass fraction Y_a is

$$\rho_{s,\alpha} = Y_\alpha \rho_s \quad (2)$$

The reaction rate is determined by Arrhenian kinetics.

$$r_\alpha(x) = \left(\frac{\rho_{s,\alpha}(x)}{\rho_s(0)}\right)^{n_\alpha} A_\alpha \exp\left(-\frac{E_\alpha}{RT_s(x)}\right) \quad (3)$$

Where: n reaction order
A_a pre-exponential factor
E_a activation energy
R universal gas constant, 8.31441 J/(K·mol)
T_s solid temperature at depth x

The chemical source term $\dot{q}_s'''$ is calculated as

$$\dot{q}_s'''(x) = -\rho_s(0) \sum_{\alpha=1}^{N_m} r_\alpha(x) H_{r,\alpha} \quad (4)$$

Where: N_m the total number of material components in the solid
$H_{r,a}$ the heat of reaction of component a

FDS solves heat transfer in solid phase according to a one-dimensional heat equation.

$$\rho_s c_{p,s} \frac{\partial T_s}{\partial t} = \frac{\partial}{\partial x}\left(k_s \frac{\partial T_s}{\partial x}\right) + \dot{q}_s''' \quad (5)$$

Where: $c_{p,s}$ specific heat capacity of the material mixture
t time
k_s thermal conductivity of the solid material mixture

The heat transfer boundary condition on the hot surface is

$$-k_s \frac{\partial T_s}{\partial t}(0,t) = h\left[T_g - T_s(0,t)\right] + \varepsilon\left[\dot{q}_r'' - \sigma T_s(0,t)^4\right] \quad (6)$$

Where: h convective heat transfer coefficient
T_g gas temperature next to the solid boundary
ε emissivity
$\dot{q}_r''$ incident radiative heat flux
σ Stefan-Boltzmann constant, $5.67032 \cdot 10^{-8}$ W/(m^2·K^4)

A similar boundary condition with appropriate change of signs could be written also to the back side of an object.

The kinetic parameters were estimated with the property estimation program coupled to Gpyro version 0.8186 (Lautenberger and Fernadez-Pello, 2009). Gpyro was set to solve the same kinetic equations as FDS. Shuffled Complex Evolution (SCE) algorithm (Duan et al., 1993) is employed in optimizations. The estimation bounds were adjusted iteratively over multiple optimizations until none of the parameters converged to the bounds.

The raw heat flow is smoothed with the method of Rath et al. (2003). The method subtracts other heat flows from baseline-corrected DSC heat flow so that only heat flows due to reactions remain visible. A dimensionless conversion a is defined as

$$\alpha(T) = \frac{m_0 - m(T)}{m_0 - m_f} \quad (7)$$

Where: m sample mass
0 subscript signifying the initial state
f subscript signifying the final state

The final mass is equal to the mass of the residual char from the pyrolysis of wood sample, i.e. $m_f = m_{char}$. The heat flow $\dot{q}_s$ consumed by heating of the sample itself is

$$\dot{q}_s = \left[(1-\alpha(T))m_0 c_{p,wood} + \alpha(T) m_{char} c_{p,char}\right]\frac{dT}{dt} \quad (8)$$

Where: $\frac{dT}{dt}$ heating rate of the DSC experiment

With a closed sample cup, the smoothed heat flow is obtained by reducing $\dot{q}_s$ from the baseline-corrected DSC signal. Without a lid, radiative exchange of the sample and the DSC furnace cannot be ignored. Radiative effects are quantified by measuring the residual char heat flow instantly after the initial measurement. The radiative heat flow $\dot{q}_{rad}$ is calculated as a difference of experimental and computational char heat flows.

$$\dot{q}_{rad} = \dot{q}_{char,exp} - \dot{q}_{char,calc} \quad (9)$$

Computational char heat flow is calculated as

$$\dot{q}_{char,calc} = m_{char} c_{p,char} \frac{dT}{dt} \quad (10)$$

With an open cup, the smoothed heat flow is obtained by reducing both $\dot{q}_s$ and $\dot{q}_{rad}$ from the baseline-corrected DSC signal.

3. Results and discussion

3.1. Thermogravimetric analysis and kinetic model estimation

Figure 2 shows the mass loss curves in thermogravimetric experiments under nitrogen for spruce at all heating rates, and its derivative (i.e. mass loss rate, MLR) in the 20 K/min experiment. The figure includes also corresponding model predictions. The figure shows the MLR of each wood primary component and the model sum as the total simulated MLR. The paper shows figures only for spruce since the results for pine are visually very similar.

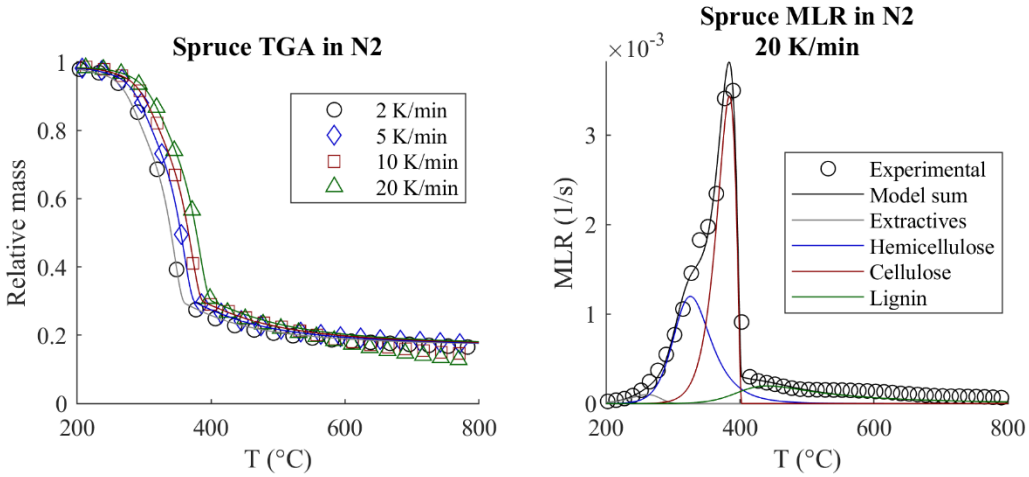

Figure 2 On left: experimental and simulated cumulative mass losses in nitrogen. On right: Experimental MLR with simulated mass loss rate of each primary component and their sum at 20 K/min. Experiments in hollow markers and simulations in continuous lines.

Mass loss begins at 200 °C in both woods. The MLR curves exhibits a shoulder at 310-350 °C and a peak at 340-385 °C, higher temperatures corresponding to higher heating rates. After the cellulosic peak, MLR decreases to low values until termination of experiment. These results are consistent with observations of Grønli et al. (2002). Air TGA results are not discussed here since oxidation is not implemented to the model at the time of writing.

Table 2 shows the reaction parameters estimated with the SCE algorithm and their estimation bounds for both spruce and pine. Component proportions excluding water are derived from dry wood composition reported by Sjöström (1981).

Table 2 Kinetic parameters and their estimation bounds.

		Parameter value (estimation bounds)				
Species	a	$Y_{s,a}(0)$ (-)	A_a (1/s)	E_a (kJ/mol)	n_a (-)	ν_{char} (-)
Spruce	Extractives	0.0167	$4.411 \cdot 10^8$ (10^6-10^{10})	107.1 (90-130)	1 (fixed)	0 (fixed)
	Hemi-cellulose	0.2785	$5.426 \cdot 10^{13}$ (10^{11}-10^{15})	168.1 (160-190)	2.5 (1-3)	0 (0-0.2)
	Cellulose	0.4103	$4.239 \cdot 10^{13}$ (10^{11}-10^{15})	195.1 (170-210)	0.62 (0.3-1.5)	0.043 (0-0.2)
	Lignin[1]	0.2696	$2.46 \cdot 10^{12}$ (fixed)	157.5 (fixed)	6.11 (fixed)	0.517 (fixed)
Pine	Extractives	0.0344	$4.957 \cdot 10^7$ (10^6-10^{10})	100.5 (90-130)	1 (fixed)	0 (fixed)
	Hemi-cellulose	0.2804	$3.194 \cdot 10^{13}$ (10^{11}-10^{15})	168.1 (160-190)	2.3 (1-3)	0 (0-0.2)
	Cellulose	0.3936	$2.146 \cdot 10^{13}$ (10^{11}-10^{15})	191.2 (170-210)	0.61 (0.3-1.5)	0.033 (0-0.2)
	Lignin	0.2726	$2.46 \cdot 10^{12}$ (10^{11}-10^{15})	157.5 (150-180)	6.11 (5-7)	0.517 (fixed)
Both	Water[2]	0.016	$9.57 \cdot 10^{22}$	136	3.31	0

[1]Values of the kinetic parameters assumed to hold identical to pine lignin.

[2]Kinetic parameters from Hostikka and Matala (2017). $Y_{s,water}(0)$ based on TGA tests in this study. Assumed to hold identical for both species.

For simplicity, a reaction order of unity was assumed for pyrolysis of both species' extractive components and their char yield was fixed to zero. When given as an optimized variable, char yield of extractives tends to converge into near-zero values. The kinetic parameters for spruce lignin were fixed to those for pine. When given as optimized variables, parameters of spruce lignin always converged to the estimation bounds.

3.2. Heat release

The heating rate settings in the MCC experiments were 20 and 60 K/min, but the device log revealed them to be actually 37.4 and 74.5 for spruce, and 33.4 and 80.6 K/min for pine, respectively. The experiments were simulated in FDS and an individual heat of combustion is fitted for each primary component. The simulations were checked to satisfy experimental heat of combustion. Table 3 collects the fitted heats of combustion. Figure 3 presents the MCC method A results of spruce and the corresponding simulations. The total heat of combustion for both woods at all heating rates is approximately 12 MJ/kg per sample mass and 14 MJ/kg per produced mass of gas, respectively. According to Method B results, the heat of complete oxidation of each wood is approximately 18 MJ/kg.

Earlier, Hostikka and Matala (2017) have obtained heats of combustion of 17.0, 13.5 and 13.4 MJ/kg for hemicellulose, cellulose and lignin, respectively for birch wood, also by fitting a simulation into MCC test results. These correspond well to the present results, except for lignin. Despite being for hardwood, the heats of combustion by Hostikka and Matala (2017) are closer to the values in the current work than the values reported in the Douglas fir pyrolysis model by Parker (1989) (10.7, 13.8 and 14.7 MJ/kg, respectively).

Table 3 Heat of combustion of wood primary components.

	Heat of combustion by component (MJ/kg)			
Species	Extractives	Hemicellulose	Cellulose	Lignin
Spruce	40	19.5	13.4	7
Pine	30	17	14	7.2

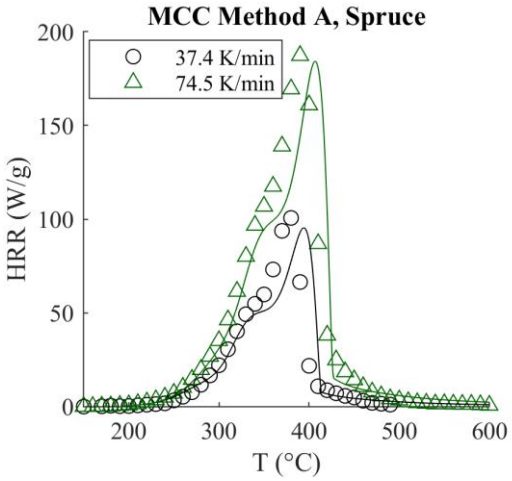

Figure 3 Experimental (hollow markers) and simulated (continuous lines) heat release rate in spruce MCC method A experiments.

3.3. Specific heat capacity and heat of pyrolysis

The linearization of average measured specific heats for both woods goes from 920 J/(kg·K) at 30 °C to 1800 J/(kg·K) at 230 °C. Specific heat capacity of wood is temperature-dependent but independent of species and density (Glass and Zelinka, 2010). The model therefore uses average specific heat of both species. Currently measured specific heats are lower than the results of Harada et al. (1998) in ambient conditions but the agreement improves in higher temperatures.

The heat of pyrolysis for each wood primary component is determined by fitting a simulation to the smoothed heat flow curve. Table 4 presents wood primary components' heats of pyrolysis and compares them to the results by Branca and Di Blasi (2016) for beech without a lid on the sample cup. Figure 4 presents the measured and simulated heat flow in the heat of pyrolysis experiments for spruce.

Table 4. Heats of pyrolysis for individual wood components and the total heat of pyrolysis determined in this work and results of Branca and Di Blasi (2016) for beech.

kJ/kg, endothermic +	With lid		Without lid		Branca, Di Blasi (2016), no lid
a	Spruce	Pine	Spruce	Pine	Beech
Extractives	0	0	0	0	
Hemicellulose	-165	-205	1250	950	247.6
Cellulose	230	148	640	600	600.7
Lignin	-1230	-1250	-1100	-1150	-922.7
Total	-249	-296	355	205	

Extractives were assigned a heat of pyrolysis equal to zero in all simulations. With the lid on, the agreement between experiments and simulation was good without specifying extractives a heat of pyrolysis. On the other hand, to achieve good agreement in simulations with an open cup, extractives should be assigned disproportionately large endothermic heat of pyrolysis. Due to uncertainty, extractives were assigned a heat of pyrolysis equal to zero also now. The similar experiments of Rath et al. (2003) on spruce wood show also endothermic heat flow before any significant mass loss. They however leave the matter undiscussed and the cause remains unclear.

Table 4 shows good consistency between currently determined cellulose and lignin heats of pyrolysis with the results of Branca and Di Blasi (2016). The only major difference is hemicellulose. Possible reasons are differences in softwoods and hardwoods and in the kinetic model, and the aforementioned uncertainties in the low-temperature region.

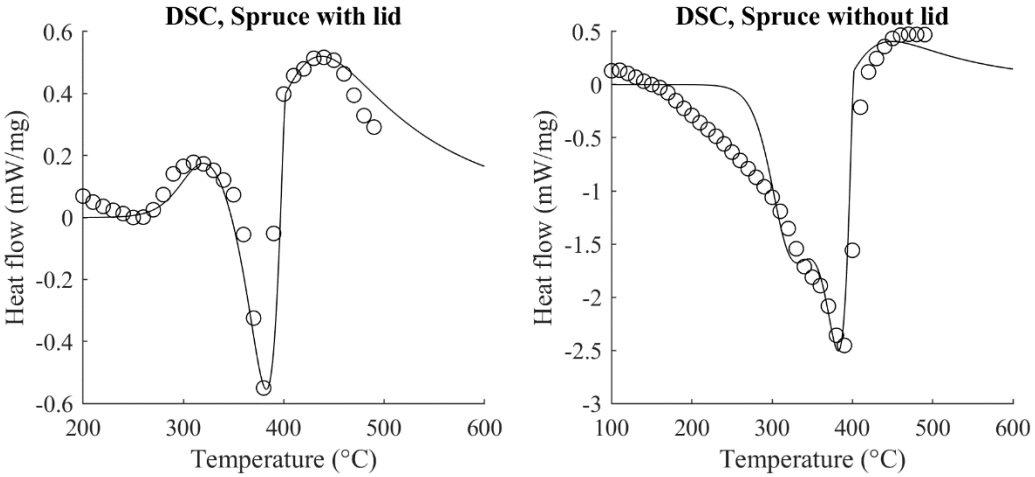

Figure 4 Experimental (hollow markers) and simulated (continuous line) heat flow in heat of pyrolysis DSC experiments for spruce. Exothermic direction is upwards.

3.4. Thermal conductivity

Measured thermal conductivities in longitudinal, radial, and tangential trunk directions are for spruce 0.191, 0.154 and 0.154 W/(m·K), and for pine, 0.259, 0.171 and 0.184 W/(m·K) respectively. The measured values for both species were slightly lower in parallel to the grain and higher in perpendicular to the grain than reported elsewhere in literature (Olek et al., 2003; Vay et al., 2015). Hankalin et al. (2009) reports radial and longitudinal conductivities of 0.08-0.1 W/(m·K) and 0.11-0.13 W/(m·K), respectively, for pine char.

3.5. Cone calorimeter

Preliminary cone calorimeter simulations are carried out. At the time of writing, material thermal properties are not optimized to fit the experiments. Therefore, simulations do not agree with the experimental results and are not shown here. These simulations already reveal the more endothermic heat of pyrolysis to give better qualitative fit to experiments. Exothermicity leads to premature and violent mass loss due to a thermal runaway.

4. Conclusions

A kinetic model for pyrolysis of Norway spruce and Scots pine, two important Nordic structural timbers, has been presented. The small scale methods of TGA, DSC and MCC show good consistency in their results, thus enabling fitting of heat of pyrolysis and heat of combustion for individual wood components. The heat of pyrolysis of extractives in open cup DSC tests is an exception due to other simultaneous unrecognized heat flows.

The current pyrolysis model predicts some mass loss and thus, heat release all the way to the end of the temperature range of TGA and MCC at approximately 800 °C. On the contrary, experimental MCC results reveals heat release to terminate at approximately 500 °C and 600 °C with the nominal heating rates of 20 and 60 K/min, respectively. Devolatilization of char residue (Várhegyi et al., 2002) was firstly investigated to model mass loss without heat release. However, after the experimental MCC signal has reached zero, the simulated value is barely above the actual detection limit of the device. Additionally, preliminary cone calorimeter simulations proved little difference between the currently presented model and the model expanded with char devolatilization. The char devolatilization reaction was therefore excluded to avoid unnecessary model complexity.

Optimization of physical properties and model validation by cone calorimeter experiments are planned as a future work. The current equipment that allows only for mass loss measurement in nitrogen atmosphere, is sufficient for optimization of material properties and validation of pyrolysis model. However, a device with capability to measure heat release is necessary to test the validity of the heat release model and to examine if the pyrolysis model needs to be supplemented by an oxidation model.

5. Acknowledgements

The authors wish to thank D.Sc. Anna Matala of VTT Technical Research Centre of Finland for conducting the MCC experiments and supporting their analysis, and Prof. Michael Gasik for helping with the conductivity measurements. The work has been funded by the Academy of Finland under grant 297030.

References

Branca, C. and Di Blasi, C., 2016. A summative model for the pyrolysis reaction heats of beech wood. *Thermochim. Acta,* **638**, pp. 10-16.

Duan, Q.Y., Gupta, V.K. and Sorooshian, S., 1993. Shuffled complex evolution approach for effective and efficient global minimization. *J. Optim. Theory Appl.,* **76**(3), pp. 501-521.

Glass, S.V. and Zelinka, S.L., 2010. Moisture Relations and Physical Properties of Wood. *Wood Handbook.* Ed. Ross R.J., Madison: USDA Forest Service, pp. 4-1 - 4-19.

Grønli, M.G., 1996. *A Theoretical and Experimental Study of the Thermal Degradation of Biomass*. Trondheim: The Norwegian University of Science and Technology.

Grønli, M.G., Várhegyi, G. and Di Blasi, C., 2002. Thermogravimetric analysis and devolatilization kinetics of wood. *Ind. Eng. Chem. Res.,* **41**(17), pp. 4201-4208.

Hankalin, V., Ahonen, T. and Raiko, R., 2009. On thermal properties of a pyrolysing wood particle. Presented at the Finnish-Swedish Flame Days, Naantali, Finland, Jan. 28-29.

Harada, T., Hata, T. and Ishihara, S., 1998. Thermal constants of wood during the heating process measured with the laser flash method. *J. Wood Sci.,* **44**(6), pp. 425-431.

Hostikka, S. and Matala, A., 2017. Pyrolysis model for predicting the heat release rate of birch wood. *Combust. Sci. Technol.,* **189**(8), pp. 1373-1393.

Lautenberger, C. and Fernandez-Pello, C., 2009. Generalized pyrolysis model for combustible solids. *Fire Saf. J.,* **44**(6), pp. 819-839.

Log, T. and Gustafsson, S.E., 1995. Transient plane source (TPS) technique for measuring thermal transport properties of building materials. *Fire Mater.,* **19**(1), pp. 43-49.

Lyon, R.E. and Walters, R.N., 2004. Pyrolysis combustion flow calorimetry. *J. Anal. Appl. Pyrolysis,* **71**(1), pp. 27-46.

Matala, A., Hostikka, S. and Mangs, J., 2008. Estimation of pyrolysis model parameters for solid materials using thermogravimetric data, *Fire Saf. Sci.*, **9**, pp. 1213-1223.

Olek, W., Weres, J. and Guzenda, R., 2003. Effects of thermal conductivity data on accuracy of modeling heat transfer in wood. *Holzforschung,* **57**(3), pp. 317-325.

Parker, W.J., 1989. Prediction Of The Heat Release Rate Of Douglas Fir, *Fire Saf. Sci.*, **2**, pp. 337-346.

Rath, J., Wolfinger, M.G., Steiner, G., Krammer, G., Barontini, F. and Cozzani, V., 2003. Heat of wood pyrolysis. *Fuel,* **82**(1), pp. 81-91.

Sjöström, E., 1981. *Wood Chemistry*. New York: Academic Press. 223 p.

Vay, O., De Borst, K., Hansmann, C., Teischinger, A. and Müller, U., 2015. Thermal conductivity of wood at angles to the principal anatomical directions. *Wood Sci. Technol.,* **49**(3), pp. 577-589.

Várhegyi, G., Szabó, P. and Antal, M.J., 2002. Kinetics of Charcoal Devolatilization. *Energy Fuels*, **16**, pp. 724-731.

Östman, B., Brandon, D. and Frantzich, H., 2017. Fire safety engineering in timber buildings. *Fire Saf. J.,* **91**, pp. 11-20.